Sensors and Materials, Vol. 33, No. 11 (2021) 4017–4030
MYU Tokyo

S & M 2742

Elimination of Motion Artifacts in Photoplethysmography Signals by Analytical Method

Hualong Guo,[1] Yang-Han Lee,[2*] Yi-Lun Chen,[2]
Shengrong Lu,[1] and Hsien-Wei Tseng[1**]

[1]College of Mathematics and Information Engineering, Longyan University, Fujian 364012, China
[2]Department of Electrical and Computer Engineering, Tamkang University, New Taipei City 251301, Taiwan

(Received July 1, 2021; accepted November 16, 2021)

Keywords: photoplethysmography (PPG), electrocardiography (ECG), independent component analysis, motion artifacts, multi-bandpass filter

Taiwan currently faces an aging population and a rise in mortality rate caused by cardiovascular disease. Therefore, the prevention of cardiovascular disease and the constant tracking of physiological information are crucial. Photoplethysmography (PPG) is used to instantaneously measure and monitor a person's physiological information. Compared with electrocardiography, PPG measurements are more convenient and less expensive. However, PPG is more susceptible to the effects of motion artifacts. To accurately analyze the physiological information contained in PPG signals, the negative effects of motion artifacts on PPG signals must first be eliminated. In this study, independent component analysis was employed to separate independent components (i.e., PPG signals and noise) from raw signals with motion artifacts. Subsequently, independent components containing PPG signals were selected and the locations of the PPG signal components in the frequency spectrum were analyzed. Next, the raw signals were passed through a multi-bandpass filter specifically designed for this study to eliminate motion artifacts. Motion artifacts were created for an experiment using two types of finger movements: vertical and horizontal finger movements. From the independent component analysis of the independent components, the waveforms of the filtered PPG signals in the time and frequency domains were acquired, which were then compared with the results of heartbeat measurement.

1. Introduction

As the standard of living rises and medical equipment and technology advance, average life expectancy continues to improve. According to the year-end demographic structure analysis conducted by the Department of Statistics of the Ministry of the Interior in 2013, the percentage of people over 65 years old continued to rise after Taiwan became an aging society in 1993. By 2013, that percentage had reached 11.53%, an increase of 2.29 percentage points from 9.24% at the end of 2003. Although population aging signifies a decline in average mortality rate, heart disease has become increasingly common; it was the fourth leading cause of death in 1996 but

*Corresponding author: e-mail: yhleepp@gmail.com
**Corresponding author: e-mail: hsienwei.tseng@gmail.com
https://doi.org/10.18494/SAM.2021.3525

ISSN 0914-4935

the second leading cause of death in 2012 according to cause-of-death statistics provided by the Department of Statistics of the Ministry of Health and Welfare.[1] The mortality rate has also increased annually. At present, the instantaneous monitoring of physiological information is a major topic of study in sports and in medical treatment.

The most well-known methods used to monitor physiological information are electrocardiography (ECG) and photoplethysmography (PPG). PPG is based on optical properties, where light changes detected by optical components are used to measure the cardiovascular system and its physiological parameters. PPG features advantages such as ease of use, diversity of measurement locations, and low cost; however, the disadvantage is that signals are prone to the effects of external interferences (artifacts). To accurately measure physiological information, the properties and composition of PPG signals must be clearly understood. The types of signals exhibiting motion artifacts and the causes of the motion artifacts must be analyzed to separate or remove the interfering signals. To address this need, in this study we proposed a method of eliminating motion artifacts.

2. Methodology

2.1 PGG

PGG is a noninvasive method used to measure physiological signals. This method involves the selection of a skin area, which is subsequently irradiated with red, green, or IR LED light, as schematically shown in Fig. 1. As the light penetrates the skin, it is deflected because of changes in the vascular caliber. Because parts of the light source are also absorbed by the blood, the light source undergoes continuous changes. Images constructed using the changing light are called PPG images. PPG signals contain information such as heart rate, respiratory rate, oxygen saturation, pulse reflection index, and pulse wave velocity.

2.1.1 Properties of PPG signals in time and frequency domains

The time domain analysis of PPG signals is commonly used to detect heartbeat frequency. As shown in Fig. 2, the distance between two wave crests is the time between heartbeats (the cardiac

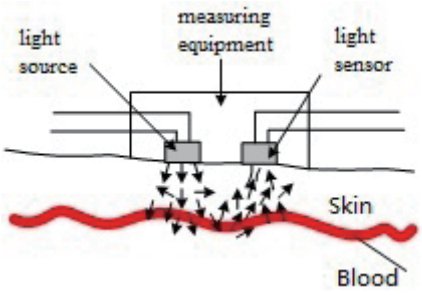

Fig. 1. (Color online) Schematic diagram of PPG signals measured by reflection measurement.[2]

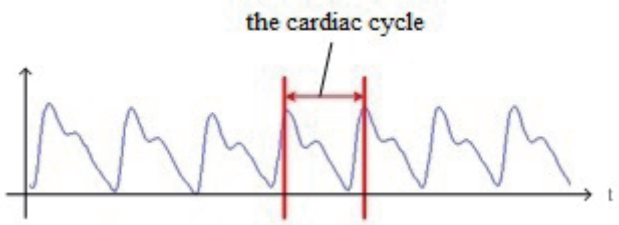

Fig. 2. (Color online) Schematic diagram of continuous PPG waveform.

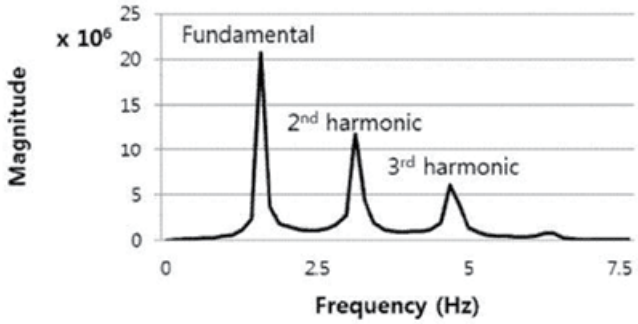

Fig. 3. (Color online) PPG signal distribution plotted as frequency spectrum.[3]

cycle). By counting the number of such distances in 1 min, the heart rate [beats per min (bpm)] is obtained.

By converting PPG signals to a frequency spectrum using the Fourier transform, physiological information such as the heart and respiratory rates can be obtained. Figure 3 shows a converted frequency spectrum featuring "clean" PPG signals (without motion artifacts); in the frequency domain, PPG signals consist of a fundamental wave, a second-harmonic wave, and a third-harmonic wave. The fundamental wave frequency can also be used to indicate the frequency of heartbeats per second. In Fig. 3, the fundamental wave crest exhibits a frequency of approximately 1.6 Hz. By multiplying the frequency by 60, an average heartbeat of approximately 96 bpm can be calculated.

2.2 Motion artifacts

When measuring PPG signals, physiological signals are prone to interference (motion artifacts) from external factors. The origins of motion artifacts vary, but can primarily be divided into poor contact with sensing elements, interference from surrounding lights, and interference from measuring instruments caused by participant movement (shaking) during measurements,[4] the last of which is the most significant.

3. Methods of Eliminating Motion Artifacts

3.1 Independent component analysis

Independent component analysis (ICA) is a statistical, computational, and linear transformation method.[5–10] ICA can be used to separate observed mixed signals into independent, non-Gaussian distributed signals. The independent signals are occasionally called the independent components of the mixed signals.

Figure 4 shows a schematic diagram of the cocktail party problem. Four people are assumed to be talking to each other simultaneously in a quiet environment, and each of them is assumed to be able to identify the sound of the listener. Concurrently, four microphones are placed in the room at various locations to collect the sounds. The mixed sounds collected by the microphones can be represented by the following mathematical equations.

$$\begin{aligned} x_1(t) &= a_{11}s_1(t) + a_{12}s_2(t) + a_{13}s_3(t) + a_{14}s_4(t) \\ x_2(t) &= a_{21}s_1(t) + a_{22}s_2(t) + a_{23}s_3(t) + a_{24}s_4(t) \\ x_3(t) &= a_{31}s_1(t) + a_{32}s_2(t) + a_{33}s_3(t) + a_{34}s_4(t) \\ x_4(t) &= a_{41}s_1(t) + a_{42}s_2(t) + a_{43}s_3(t) + a_{44}s_4(t) \end{aligned} \tag{1}$$

Here, a_{11}, a_{22}, ..., a_{44} are the weighted parameters of the distance between the microphones and the sources of the sounds.

3.1.1 Basic definition of ICA

In general, signals collected during signal collection are mixed signals, where the patterns of the mixed and raw signals are unknown. The raw signal is typically difficult to identify. However, ICA is able to separate the raw signal $s(t)$ from the mixed signal $x(t)$ when $x(t)$ is known. The basic model equation for ICA is as follows:

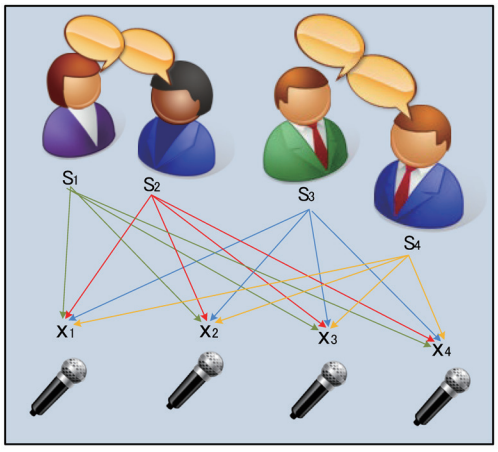

Fig. 4. (Color online) Schematic diagram of cocktail party problem.

$$x(t) = \begin{bmatrix} x_1 \\ x_2 \\ x_3 \\ \vdots \\ x_m \end{bmatrix} = \begin{bmatrix} a_{11} & a_{12} & a_{13} & \cdots & a_{1n} \\ a_{21} & a_{22} & a_{23} & \cdots & a_{2n} \\ a_{31} & a_{32} & a_{33} & \cdots & a_{3n} \\ \vdots & \vdots & \vdots & \ddots & \vdots \\ a_{m1} & a_{m2} & a_{m3} & \cdots & a_{mn} \end{bmatrix} \begin{bmatrix} s_1 \\ s_2 \\ s_3 \\ \vdots \\ s_n \end{bmatrix} = \mathrm{A}s(t), \tag{2}$$

where A is an $m \times n$ mixing matrix that represents the weighted parameters between the observed mixed signal $x(t)$ and the original independent signal $s(t)$.

3.1.2 Actual and simulation examples

As reported in this section, actual examples of mixed signals and those created from simulations were used, and changes in mixed signals were calculated by ICA. Results of the simulated mixed signals are shown in Fig. 5.

Figures 5(a1)–(a3) show the original independent signals, which comprised sine, square, and triangle waves, respectively. Figures 5(b1)–(b3) show the mixed signals, which consist of mixtures of sine and square waves, square and triangle waves, and sine and triangle waves, respectively. Figures 5(c1)–(c3) show the results after ICA was used; the output signals reveal the characteristics of the sine, square, and triangle waves, respectively.

Following the above simulation, actual PPG signals were analyzed. As shown in Fig. 6, these PPG signals were mixed with motion artifacts (created by vertical finger movements), which are superimposed on the frequency spectrum. The components with different frequencies were then separated by ICA.

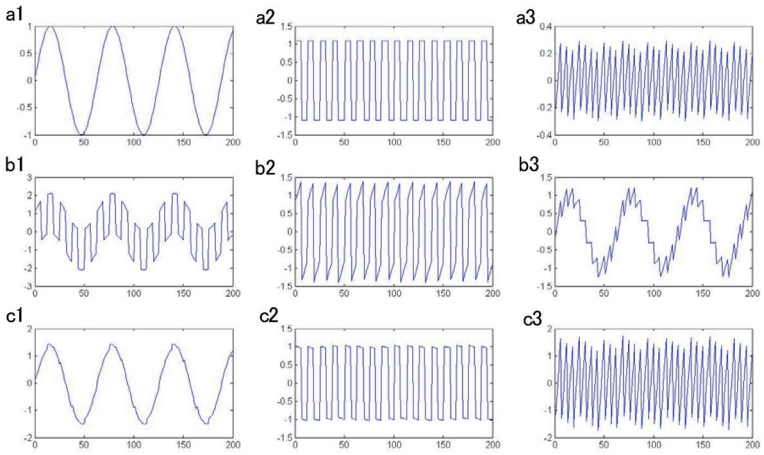

Fig. 5. (Color online) ICA simulation results.

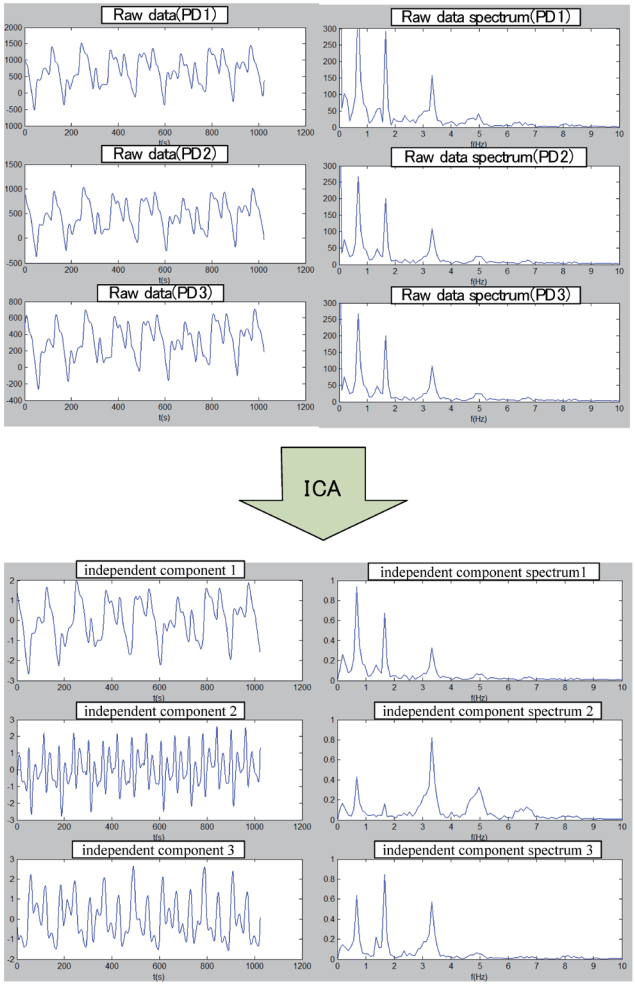

Fig. 6. (Color online) Results of ICA performed on actual PPG signals.

3.2 Correlation coefficient

The correlation coefficient is a statistical indicator designed by Karl Pearson used to reflect the correlation between variables. From a statistical perspective, the correlation coefficient measures the "distance from independence" between two variables. The correlation coefficient is calculated using the product–moment method, where the two variables and their mean deviation are used as the basis of calculation. The correlation between the two variables is obtained by multiplying the two mean deviations. For example, the correlation coefficient ($\rho_{X,Y}$) of variables X and Y is

$$\rho_{X,Y} = \frac{\operatorname{cov}(X,Y)}{\sigma_X \sigma_Y}, \tag{3}$$

where cov(X, Y) is the covariance of X and Y, and σ_X and σ_Y are the standard deviations of X and Y, respectively.

In the methods employed in this study, correlation coefficients were used to select the independent components. The correlation between the analyzed independent components and the PPG signals without motion artifacts was studied using the frequency spectrum. The independent component with the greatest correlation coefficient was chosen as the primary component. Figure 7 shows the correlation coefficients between PPG signals without motion artifacts and independent components 1, 2, and 3, which were 0.1549, 0.1519, and 0.5278, respectively. Because independent component 3 featured the highest correlation, it was selected for subsequent analysis.

3.3 Spectrum analysis

Information concerning the analysis of PPG signals on the frequency spectrum was described previously. The PPG signals on the frequency spectrum are composed of fundamental and harmonic waves. To obtain clean PPG signals, the frequency and location of the fundamental and harmonic waves must first be identified. However, signals contaminated by motion artifacts cause misjudgment of the frequency and location of the fundamental and harmonic waves. Therefore, in the two previous sections, the correlation coefficients between the PPG signals and the independent components were analyzed and compared by ICA and the frequency domain method, after which the desired independent components were effectively separated. As reported in this section, a simple method was designed to determine the peak frequencies of the fundamental and harmonic waves.

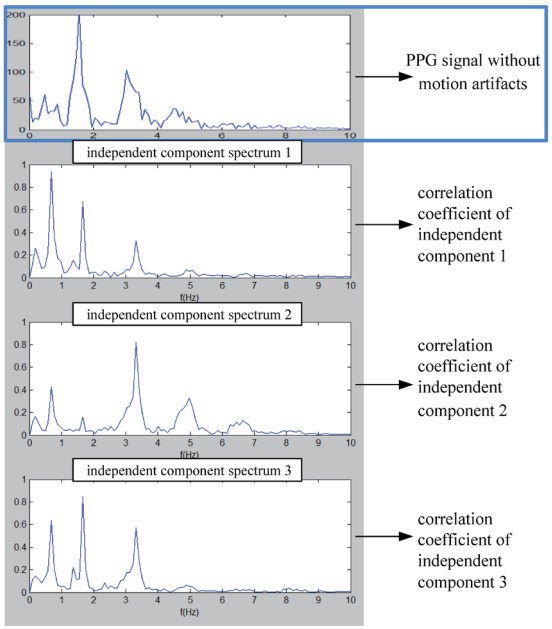

Fig. 7. (Color online) Comparison between correlation coefficients of three independent components.

The procedure of this method is shown in Fig. 8. First, the maximum value in the 0.5–5 Hz frequency band was identified. Subsequently, the peak frequency f_1 of the fundamental wave was obtained. Next, using the characteristics of the harmonic waves, the frequency region of f_1 was expanded by a factor of 2–3 to attain the maximum value in this region. The detection ranges were $2f_1 \pm 0.3$ Hz and $3f_1 \pm 0.3$ Hz. The detected peak frequencies are shown in Fig. 9.

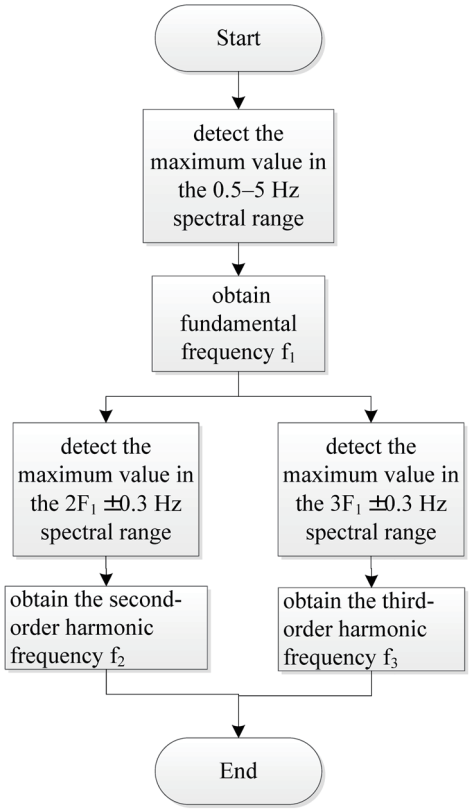

Fig. 8. (Color online) Procedure for detecting peak frequencies of fundamental wave and second and third harmonic waves.

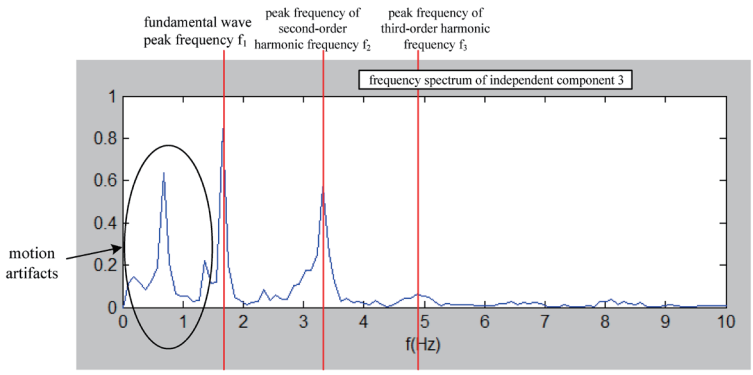

Fig. 9. (Color online) Schematic diagram of detected peak frequencies.

After acquiring the peak frequencies of the fundamental wave and the second- and third-harmonic waves, the components of these three waves were extracted using a multi-bandpass filter, which was designed to extract the fundamental and harmonic waves from the original PPG signals.

3.4 Heart rate detection algorithm

When reading PPG signals, the current heart rate can be determined by calculating the time difference between two wave crests. Therefore, to obtain accurate heart rate information, the precise detection of the locations of the wave crests is required. The crest detection algorithm developed in this study was based on the bigger fall side method proposed by Navakatikyan *et al.* in 2002[11,12] and the improved methods proposed by Chen in 2004.[13] The idea was inspired by the fact that wave crests and troughs have the widest gap in a waveform. By observing complete PPG waveforms, no turning points were found between the wave troughs and the adjacent crests, and the vertical distance between the two extrema was the greatest. Therefore, by detecting all of the extrema in a PPG waveform, calculating the differences between the extrema, and setting a determination condition to detect the locations where the greatest difference occurred, the locations of the wave crests and troughs can be identified.

4. Experimental Results

4.1 Experimental equipment and procedure

In this study, a reflective PPG measurement method was adopted. In the experiment, measurements were performed at the tip of an index finger, as shown in Fig. 10. A green LED emission light was used for analysis. Three light sensors were installed on the device for light reception. The three light sensors simultaneously collected the green LED light that was reflected after transmitting through the finger, which produced three original data points for analysis. The sampling frequency of the measuring device was set at 100 Hz, and the experimental platform MATLAB was used for simulation analysis.

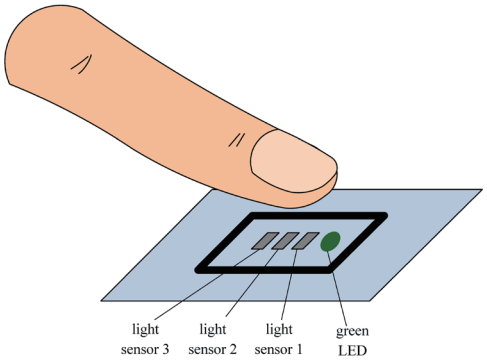

Fig. 10. (Color online) Schematic diagram of PPG measuring device.

In the experiment, two types of continuous motion artifacts were produced using vertical and horizontal finger movements. Two experiments were performed for each type of movement.

4.2 Experimental scenarios and results of analysis

4.2.1 Vertical finger movement

The three original PPG signals are shown in Fig. 11. The left side of the diagram shows the waveform observed in the time domain and the right side shows the corresponding frequency spectrum.

The original PPG waveform diagram shows the significant effect of motion artifacts on the PPG waveform. Because the corresponding frequency of the heart rate component "peak frequency of the fundamental wave" could not be identified on the frequency spectrum, ICA was employed to separate the independent components from the raw signals (Fig. 12).

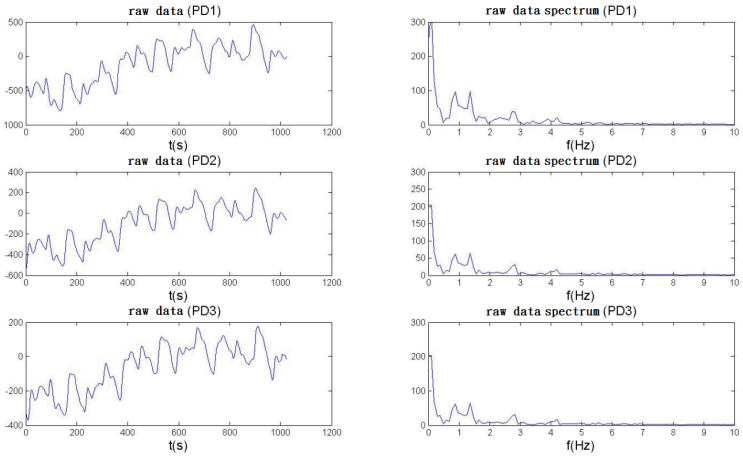

Fig. 11. (Color online) Raw measurement signal (vertical finger movement).

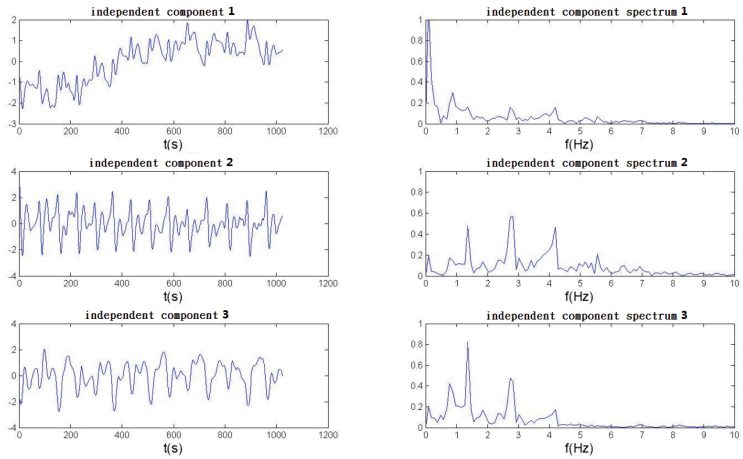

Fig. 12. (Color online) Three independent components obtained by ICA (vertical finger movement).

Once the frequency composition of the PPG signals was identified, a multi-bandpass filter featuring the same frequency was designed. Subsequently, original data were inserted into the filter to eliminate motion artifacts, as shown in Fig. 13.

The algorithm described in Sect. 3.4 was used to compute the processed PPG signals to calculate heart rate information, as shown in Fig. 14.

4.2.2 Horizontal finger movement

An experiment was performed to analyze the measurement of horizontal finger movement, which was carried out by the same process as that used for the vertical finger movement. Once the frequency composition of the PPG signals was identified, a multi-bandpass filter featuring the same frequency was designed. Subsequently, the original data were inserted into the filter to eliminate motion artifacts, as shown in Fig. 15.

The algorithm described in Sect. 3.4 was used to compute the processed PPG signals to calculate heart rate information, as shown in Fig. 16.

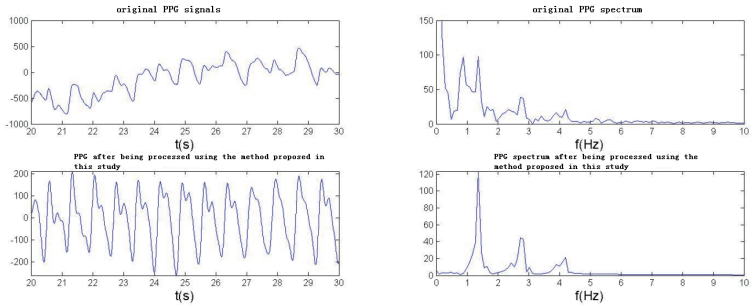

Fig. 13. (Color online) Original PPG signals and PPG signals after processing (vertical finger movement).

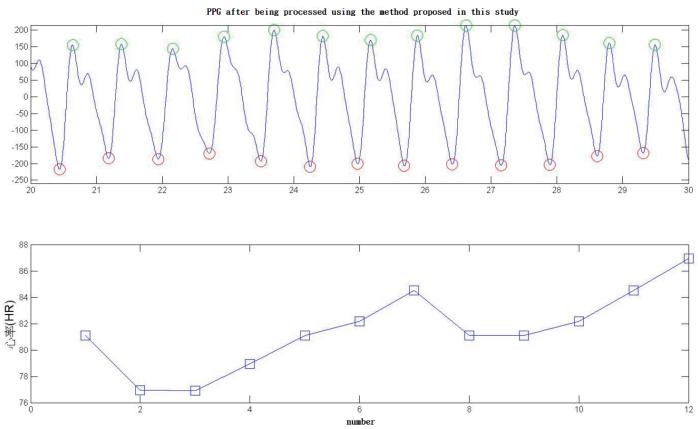

Fig. 14. (Color online) Heart rate detection results (vertical finger movement).

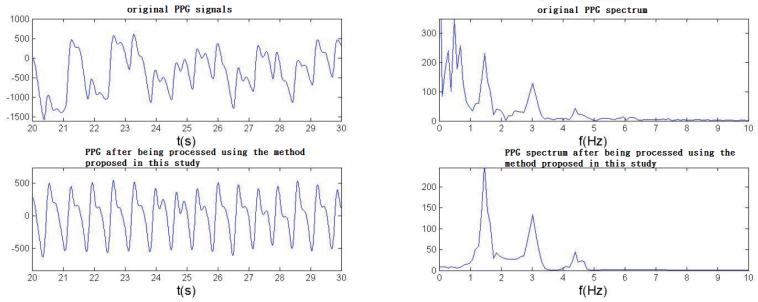

Fig. 15. (Color online) Original PPG signals and PPG signals after processing (horizontal finger movement).

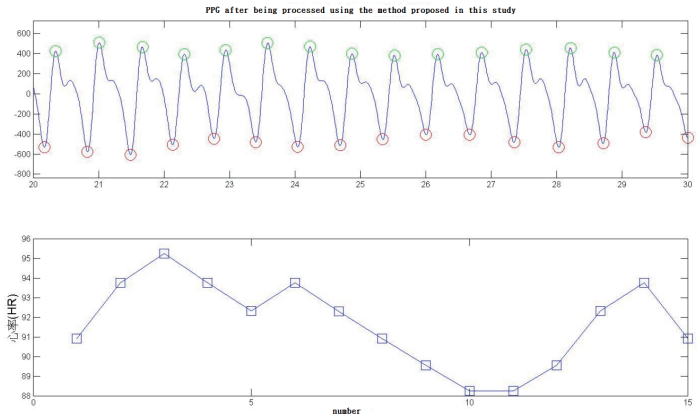

Fig. 16. (Color online) Heart rate detection results (horizontal finger movement).

4.3 Experimental data results

The average heart rates measured by ECG were set as the reference. Next, the average heart rates obtained from the experimental analysis of the PPG signal were compared with the reference, as shown in Table 1. The experimental results indicated that the proposed method of analysis can effectively eliminate the motion artifacts of PPG signals and produce favorable waveforms. Therefore, when waveform information is complete, heart rate detection is very precise. The integrated data in Table 1 show that the differences between the average heart rates

Table 1
Comparison between average heart rates measured by ECG and those obtained by experimental analysis of PPG signals.

		Average heart rate (bpm) measured by ECG	Average heart rate (bpm) measured by PPG	Difference in average heart rate (bpm) between ECG and PPG	Percentage difference (%)
Vertical finger movement	E 1	82.3	81.5	−0.8	0.97
	E 2	82.8	82	−0.5	0.6
Horizontal finger movement	E 1	88.3	89.7	+1.4	1.59
	E 2	91.6	92.1	+0.5	0.55

obtained from PPG and ECG waveforms ranged between 0.55 and 1.59%, indicating that the heart rates obtained from the PPG waveforms were almost identical to those obtained from the ECG waveforms. Concerning other factors that affect physiological information, such as the varying time of signal transfer and body movements, we concluded that the error rates of the average heart rate between PPG and ECG were all within a reasonable range.

5. Conclusion and Future Prospects

PPG is used in a wide range of applications. In general, when using this method to analyze physiological information, the patient's body must remain stationary. When movements occur during PPG measurement, PPG is prone to interference. Furthermore, the resulting waveforms are affected, making analysis difficult. For example, interference with waveforms causes an inaccurate detection of the heart rate, the most crucial physiological information. In certain scenarios, analysis is severely affected, rendering waveform analysis impossible. Therefore, a method of eliminating motion artifacts was proposed in this study. A simulation-based experiment demonstrated the validity of the proposed method. From the experimental results, the average heart rate difference between PPG and ECG ranged from 0.55 to 1.59%. This demonstrates that the information of PPG interference obtained via the proposed analytical method can be effectively filtered out of the interference.

The simulation in this study was performed using MATLAB on a computer; in future studies, instant, real-time processing should be implemented practically in the field of medical treatment and fitness equipment such as treadmills. However, in the real-time analysis, there are many factors that need to be re-examined and designed; thus, there is a wide scope for further development of the proposed method.

Acknowledgments

The works are supported by the Great project of production, teaching, research of Fujian provincial science and Technology Department (2019H6023), supported by Longyan Science and Technology Project (2019LYF12010), Longyan University's Qi Mai Science and Technology Innovation Fund Project of Liancheng ([2018]132), and Shanghang (2019SHQM05) County, Longyan and Longyan University's Research and Development Team Fund ((2018)8), and the Ministry of Science and Technology, Taiwan, project of MOST 110-2221-E-032 -018 -MY2 and the Ministry of Education, Taiwan, project of "Agriculture Artificial Intelligence Internet of Things (AgAIoT)".

References

1 Department of Statistics, Ministry of Health and Welfare: The 2012 Statistical Yearbook on Causes of Death, http://www.mohw.gov.tw/cht/DOS/DisplayStatisticFile.aspx?d=13718&s=1 (accessed June 2014).
2 A. V. Challoner and C. A. Ramsay: Phys. Med. Biol. **19** (1974) 317. https://doi.org/10.1088/0031-9155/19/3/003
3 J. M. Cho, Y. K. Sung, K. W. Shin, D. J. Jung, Y. S. Kim, and N. H. Kim: 2012 IEEE-EMBS Conf. Biomed. Eng. Sci. (IEEE, 2012) 28–33. https://doi.org/10.1109/IECBES.2012.6498141

4 Q. Z. Cai: PPG Motion Artifact Detection and Signal Reconstruction, Master's Thesis, Department of Automatic Control Engineering, Feng Chia University (2009).
5 C. Jutten and J. Herault: Signal Process. **24** (1991) 1. https://doi.org/10.1016/0165-1684(91)90079-X
6 E. Vincent, S. Araki, F. Theis, G. Nolte, P. Bofill, H. Sawada, A. Ozerov, V. Gowreesunker, D. Lutter, and N. Q. K. Duong: Signal Process. **92** (2012) 1928. https://doi.org/10.1016/j.sigpro.2011.10.007
7 P. Comon: Signal Process. **36** (1994) 287. https://doi.org/10.1016/0165-1684(94)90029-9
8 D. J. Bouveresse and D. N. Rutledge: Data Handling Sci. Technol. **30** (2016) 225. https://doi.org/10.1016/B978-0-444-63638-6.00007-3
9 Te-Won Lee, A. Ziehe, R. Orglmeister, and T. Sejnowski: Proc. 1998 IEEE Int. Conf. Acoustics, Speech and Signal Processing, ICASSP '98 (IEEE, 1998) 1249–1252. https://doi.org/10.1109/ICASSP.1998.675498
10 S. Amari: Neural Comput. **10** (1998) 251. https://doi.org/10.1162/089976698300017746
11 M. A. Navakatikyan, C. J. Barrett, Geoffrey A. Head, J. H. Ricketts, and S. C. Malpas: IEEE Trans. Biomed. Eng. (2002) 662. https://doi.org/10.1109/TBME.2002.1010849
12 G. M. Friesen, T. C. Jannett, M. A. Jadallah, S. L. Yates, S. R. Quint, and H. T. Nagle: IEEE Trans. Biomed. Eng. (1990) 85. https://doi.org/10.1109/10.43620
13 C. H. Chen: The Study of the Variation Trend for Diastolic Pressure of the Surgical Patients utilizing Non-Invasive Plethysmography Signal, Department of Mechanical and Electromechanical Eng., National Sun Yat-sen University (2004).